A Proton Imaging System for Magnetic Proton Recoil Neutron Spectrometer

Zhang Jianfu, Zhang Xianpeng, Ruan Jinlu, Yang Shaohua, Liu Jinliang, Chen Liang, Liu Linyue, Ma Jiming

State Key Laboratory of Intense Pulsed Radiation Simulation and Effect (Northwest Institute of Nuclear Technology), Xi'an, 710024, China

ABSTRACT

Magnetic proton recoil (MPR) neutron spectrometer is considered as a high-performance instrument to measure deuterium-tritium (DT) neutron energy spectrum in magnetic confinement fusion, inertial confinement fusion experiments and other fusion devices. A compact proton imaging system (PIS) has been developed for MPR neutron spectrometer. The PIS was used as focal plane detector (FPD) to detect and image the fluence distribution of recoil protons. The PIS consists of a thin plastic scintillator, fiber optic taper and image guide, electron-multiplying charge-coupled device (EMCCD) and data acquisition system. The key imaging properties, including resolution, response to proton and capability as a FPD for the MPR neutron spectrometer, were evaluated using proton beams at accelerators. The PIS with Gd_2O_2S:Tb scintillator screen has higher performance in resolution and light yield than that with 2 mm plastic scintillator. The Gd_2O_2S:Tb scintillator screen can be used as an ideal candidate for proton imaging. The imaging properties of the PIS shown in this paper have demonstrated that the PIS is suitable for the MPR spectrometer in DT neutron measurement.

Keywords: MPR neutron spectrometer, proton imaging system, Gd_2O_2S:Tb scintillator screen, thin plastic scintillator, light yield, spatial resolution

1. Introduction

Magnetic proton recoil (MPR) neutron spectrometer is considered as a high-performance instrument to measure deuterium-tritium (DT) neutron energy spectrum in magnetic confinement fusion (MCF), inertial confinement fusion (ICF) experiments and other fusion devices [1–5]. The method of MPR is based on n-p elastic scattering and magnetic dispersion. Neutrons are converted to protons through n-p elastic scattering in the polyethylene (CH_2) foil. In the magnetic field of the MPR neutron spectrometer, the recoil protons are spatially separated according to their momentum and then focused on the focal plane detector (FPD) which records the spatial position of each recoil proton. Thus, the recoil proton energies distribution can be converted into a position distribution. The FPD for the MPR neutron spectrometer has to meet the requirement of a good position resolution, proton response and signal to background. Currently, measurements of recoil proton distribution for the MPR neutron spectrometer are performed using CR-39 track detectors or scintillation detector array. CR-39 is a plastic which is sensitive to appropriate energy charge particle as a track detector. It has 100% detection efficiency for protons less than 8 MeV. This kind of detector has been widely used as FPD in many ICF experiments [4,6,7]. However, CR-39 detector is quite time

consuming and difficult to implement since it needs to be etched, photomicrographed and digitized. The scintillation detector array called hodoscope has been applied as FPD in many MCF experiments [8-10]. The hodoscope based on the phoswich technique is less sensitive to background by working in counting mode of high frequency. The hodoscope is composed of an array of 32 plastic scintillators each connected to one photomultiplier tube. It has been upgraded to get better signal to background by each plastic scintillator connected to two photomultiplier tubes.

In this work, a proton imaging system (PIS) was developed as FPD for the MPR neutron spectrometer. The PIS can be considered as a position sensitive proton detector based on proton imaging method. The PIS will work with light integrating mode in real time. This paper describes the PIS configuration and presents some imaging properties measured using proton beams. The Gadolinium Sulphate Oxide doped with Terbium (Gd_2O_2S:Tb) scintillator screen (typically used in X-ray image converters) for proton imaging application is discussed by comparing its performance to thin plastic scintillator in terms of spatial resolution and light yield.

2. PIS design

The main objective is to design PIS that can record the proton distribution by achieving two-dimensional proton imaging under the condition of the MPR neutron spectrometer. Figure 1 is a schematic of the PIS for the MPR neutron spectrometer. The PIS consists of a thin plastic scintillator, fiber optic taper and image guide, electron-multiplying charge-coupled device (EMCCD) camera and data acquisition system. The EMCCD is based on standard CCD with the addition of a gain register, which allows the signal electrons to be multiplied with lower noise. The EMCCD camera used in this design is based on a back-illuminated CCD201 from E2V technologies. In the PIS, the thin plastic scintillator is used to efficiently convert the protons to visible light. The light escapes from the surface of scintillator can be conveyed through the relay optical system to the EMCCD camera of high spatial resolution (1000×1000, 13μm square pixel) and further processed by image data acquisition system to form a digital image. The digital image can be used to determine the distribution of protons.

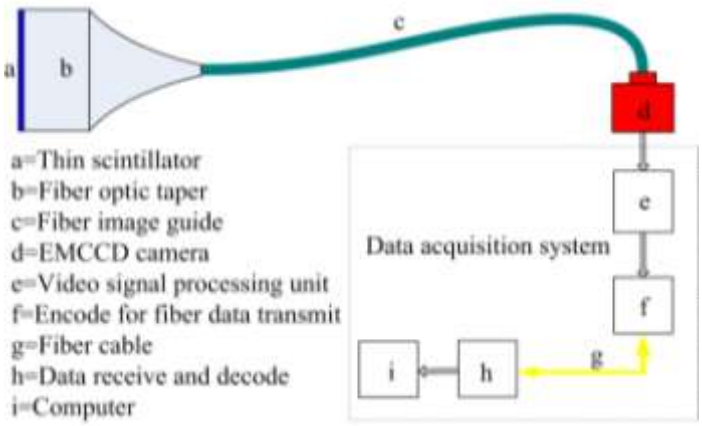

Fig. 1. Sketch of the PIS to be used for FPD on the MPR neutron spectrometer.

Plastic scintillators have been widely used for charged particle detection because of their fast time response, high light yield and favorable mechanical properties. It is easy to fabricate in large area and any shape. In the scintillator plate, the scintillation light is emitted in all directions. The light photon will be reflected back if its angle of incidence is larger than critical angle. The light spreading dimension depends on the reflection angle and the thickness of scintillator. The use of array of scintillating fibers can prevent resolution loss due to light spreading. In principle, the spatial resolution obtained with thin plastic scintillator is degraded because of the increased light spread distribution compared to array of scintillating fibers. Since 14 MeV protons will be completely stopped within plastic scintillator about 2 mm thickness, a simple thin plastic scintillator is reasonable for proton imaging instead of array of scintillating fibers for PIS.

In the PIS, the fiber optical system is composed of a fiber optic taper (tapering ratio3.3:1) and a fiber image guide (diameter of 1 cm) replacing a mirror and a lens. Fiber optical system coupling is usually more efficient than a lens. For this application, the EMCCD is equipped with a fiber optic window, which is used to directly couple to fiber image guide. The fiber optic taper is used to increase the effective detection area of the PIS. To avoid radiation damage to the EMCCD sensor, the EMCCD camera will be located far from the irradiation by using a long fiber image guide. Because of the distance and shielding, the EMCCD camera is able to obtain images with little background from irradiation.

An image data acquisition system (DAC) for protons imaging was developed [11]. In present work, the DAC based on fiber communication and the standard USB transfer is employed. EMCCD video signals are digitized and transmitted to long-distance acquisition hardware through fiber cables, and the raw digital images are stored on the memory installed in the computer. The terminal of DAC can be placed in the measurement room to control the EMCCD camera by fiber cables of several tens meters.

3. Experiment and results

3.1. Resolution measurement

The resolution measurement was performed with proton beams from the 2×6 MV tandem accelerator at Peking University. In the experiment, the proton beam was defocused at the end of the beam line with the beam intensity of several tens pA. During the measurement, the accelerator was operated in a continuous mode and the proton beam was delivered through a Ti film window of ϕ10 mm diameter and 5 μm thickness with a frequency of 50 Hz. The proton beam at the energy 10 MeV was selected. The line spread function (LSF) provides a detailed description of the spatial resolution. The tungsten (W) edge image is usually used to measure the LSF of imaging system. In the measurement, the W edge was placed between the Ti window and the scintillator with the edge aligned along the proton beam line. The digital W edge image was derived as the following. First, each image was smoothed with a 2-D median filtering to suppress little high frequency noise. The filtered image was then corrected by subtracting the average background of readout noise. The background image was measured without any protons (dark current image). Line profile perpendicular to the W edge image was averaged to get the edge spread function (ESF). The LSF was then obtained by differentiating

the ESF.

Gd_2O_2S:Tb scintillator screens are typically used in X-ray image converters. It has excellent scintillation properties such as high light yield and good resolution. Gd_2O_2S:Tb scintillator screen used for the PIS consists of a reflecting layer and a phosphor layer of 0.2 mm thickness. To test its applicability for proton imaging, the spatial resolution of Gd_2O_2S:Tb scintillator screen (FWHM of LSF) was first evaluated by comparing to thin plastic scintillator. Figure 2 (a) and (b) show the background-subtracted W edge image recorded with the PIS, using the 2 mm plastic scintillator and Gd_2O_2S:Tb scintillator screen, respectively. Fig. 2(c) shows the comparison of the LSFs of the PIS. The two FWHMs calculated from the LSFs were estimated to be 0.95 mm and 0.72 mm, respectively for 2 mm plastic scintillator and Gd_2O_2S:Tb scintillator screen. The result presented here shows an improvement in spatial resolution with Gd_2O_2S:Tb scintillator screen.

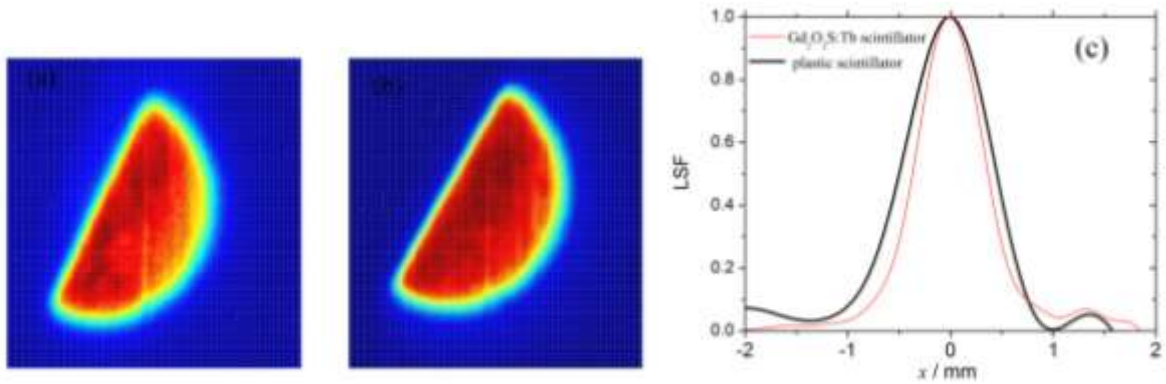

Fig. 2. The background-subtracted W edge image recorded with the PIS, (a) 2 mm plastic scintillator, (b) Gd_2O_2S:Tb scintillator screen; (c) Comparison of the LSFs of the PIS with 2 mm plastic scintillator Gd_2O_2S:Tb scintillator screen using the proton beam at 10 MeV.

3.2 Response to protons

Light yield of the scintillator detected by the PIS should be linear to proton intensity so that the proton fluence distributions can be measured. Response to protons of the PIS allows us to evaluate its applicability for determining the proton fluence. The response to protons was also performed with proton beams of 10 MeV at the 2×6 MV tandem accelerator. Response to protons of the PIS working in light integrating mode is defined by the average gray values (AGV) on each pixel per unit proton fluence. Response to protons was obtained by measuring the gray values of the image varying with the proton fluence. The AGV of image represents light yield of the scintillator detected by the PIS over the EMCCD integration time. The beam intensity was monitored by a Faraday cup detector of 3 cm^2 and the proton fluence was normalized by the integration time of the PIS. The typical integration time of the EMCCD in the measurement was 150 ms. The internal gain of the EMCCD camera was set to get the desired image according to the beam intensity.

Response to protons of the PIS with Gd_2O_2S:Tb scintillator screen and 2 mm plastic scintillator was measured at 10 MeV proton. The internal gain of the EMCCD with the Gd_2O_2S:Tb scintillator screen and 2 mm plastic scintillator was set to EM=1 and EM=80, respectively. This reduction of internal gain is due to the high light yield of the Gd_2O_2S:Tb

scintillator screen. The internal gain ratio of 69 (EM=80/EM=1) was measured to correct the gray values. Figure 3 presents AGV of the image (EM=1) as a function of proton fluence. Linear best fit the measured data, meaning that the outputs of AGV are proportional to the proton fluence. The response to protons of the PIS with the Gd_2O_2S:Tb scintillator screen and 2 mm plastic scintillator are 300 and 13 AGV/proton (EM=1), respectively. It can be adjusted by setting the EMCCD camera with different internal gain. Response to protons of the PIS with Gd_2O_2S:Tb scintillator screen is about 23 times higher than that with 2 mm plastic scintillator at 10 MeV protons.

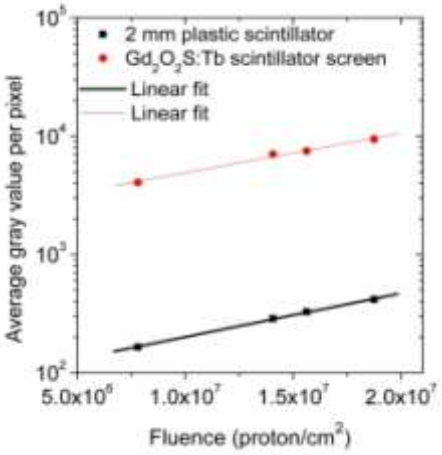

Fig. 3. Average gray value of the images (EM=1) as a function of proton fluence at 10 MeV.

3.3 Testing on MPR neutron spectrometer

In order to evaluate the performance of the PIS using for the MPR neutron spectrometer, a test using proton beam was carried out at the HI-13 tendon accelerator at China Institute of Atomic Energy (CIAE). In the test, the PIS acted as the FPD of the MPR neutron spectrometer. The protons was closely Gaussian in shape and had a FWHM of 90 keV energy spread at the energy of 14.3 MeV before entering into the proton collimator with width of 2 mm. Then the protons were allowed to enter into the magnetic part of the MPR spectrometer. The protons in the magnetic field were momentum analyzed and focused on the focal plane. The proton distribution was finally recorded by the PIS with 2 mm plastic scintillator and Gd_2O_2S:Tb scintillator screen, respectively. The effective detection area of the PIS was increased to cover a lager proton energy range by using a fiber optic taper of 7:1.1 cm. The protons exit of vacuum chamber was made of a thin Ti window of 100μm thickness and 80 mm in diameter, which allows the PIS to obtain precise position determination of the protons outside the vacuum chamber.

Figure 4 (a) and (b) show the raw digital images of the proton distribution detected by the PIS, from which the FWHMs can be obtained. Figure 4(c) compares the profiles of the image (a) and (b), normalized to peak height. The FWHMs of the position resolution are estimated to be 4.4 mm and 4.3 mm respectively for plastic scintillator and Gd_2O_2S:Tb scintillator screen. The dispersion on the focal plane of the MPR neutron spectrometer is ~40 keV/ mm. The energy resolutions, including the proton energy spread and magnetic field

spread, result in the FWHMs of 176 keV and 172 keV, respectively. Moreover, the MPR neutron spectrometer typically works with energy resolution larger than 2% (~280 keV FWHM) for measuring DT neutrons. Thus, the resolution of the PIS has little effect on the resolution of the MPR neutron spectrometer. The PIS with Gd_2O_2S:Tb scintillator screen allows better quality of proton imaging to be achieved.

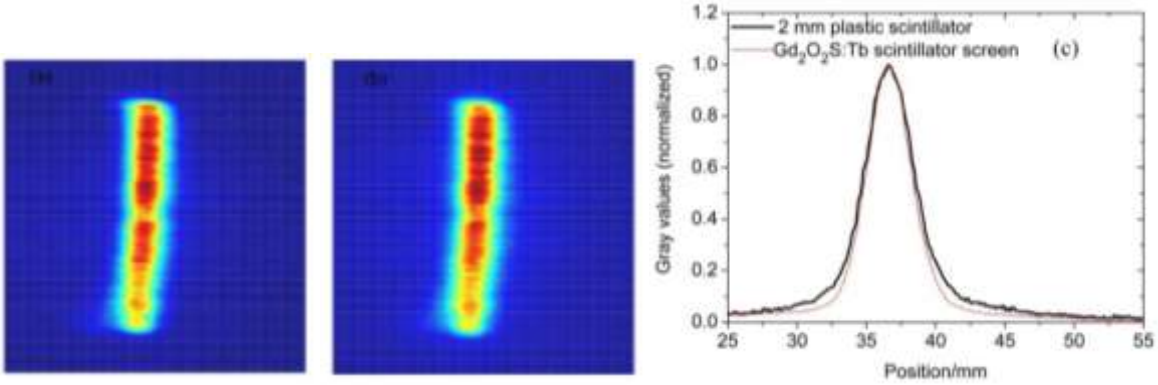

Fig. 4. The raw digital images of the proton distribution detected by the PIS, (a) Gd_2O_2S:Tb scintillator screen, (b) 2 mm plastic scintillator; (c) comparison of the horizontal line profiles of the images with 2 mm plastic scintillator and Gd_2O_2S:Tb scintillator screen.

4. Discussions

We have preliminarily tested some performances of the PIS with 2 mm plastic scintillator and Gd_2O_2S:Tb scintillator screen. Since it is used to detect the proton distribution under the condition of the MPR neutron spectrometer, the PIS will suffer irradiation from the background (e.g. scattering neutrons and gamma rays) and generate background image. Thin plastic scintillator has low sensitivity to background because of the low detection efficiency. If the range of particles produced by background is larger than the thickness of scintillator, the energy deposited in the thin scintillator will be less than the full energy of neutrons. In addition, the resolution of the PIS becomes degraded due to the spread of the light generated in the thicker scintillator. To obtain better resolution and suppress more background, the thickness of scintillator should be as thin as possible. However, for 14 MeV recoil protons, if the scintillator thickness is less than 2 mm, they will also not deposit their entire energy to achieve the best signals. So there exists an optimum thickness of the thin plastic scintillator according to practical application.

The Gd_2O_2S:Tb scintillator screen has the capability to convert the protons to visible light with maximum quantum efficiency around 545 nm, matching the peak in the quantum efficiency of the EMCCD. Thus, the use of Gd_2O_2S:Tb scintillator screen can improve quantum efficiency. Due to its effective thickness of 0.2 mm, the Gd_2O_2S:Tb scintillator screen can also provide higher resolution for proton imaging applications. Obviously, The Gd_2O_2S:Tb scintillator screen is more suitable for the PIS in spatial resolution and light yield comparing to 2 mm plastic scintillator. The PIS used in this paper can meet the requirement of the MPR neutron spectrometer in resolution and proton response. For higher resolution applications, array of scintillating fibers might be better choice. However, the economic and technical factors of large area structured crystals should be concerned.

5. Conclusion

In this paper, a PIS has been developed to detect recoil proton distribution for the MPR neutron spectrometer. Thin plastic scintillator and Gd2O2S:Tb scintillator screen were used for proton imaging instead of array of scintillating fibers. The use of thin scintillator and fiber optical coupling system makes the PIS a compact, simple in structure and more efficient FPD. The main imaging properties of the PIS were evaluated using proton beam and the PIS used as a FPD for the MPR neutron spectrometer was tested. Due to its high performances in spatial resolution and light yield, Gd_2O_2S:Tb scintillator screen can be used as an ideal candidate for proton imaging. The imaging properties of the PIS shown in this paper have demonstrated that the PIS is suitable for the MPR spectrometer in DT neutron measurement. Further improvements will be focused at allowing the PIS to work in photon-counting mode.

Acknowledgements

This work is supported by the National Natural Science Foundation of China (Grant No. 11175141 and 11275153). We would like to thank the staffs in the HI-13 tandem accelerator laboratory at CIAE and the staffs in the 2×6 MV tandem accelerator at Peking University. The authors are also grateful to Dan Su, Xichao Ruan and Long Hou at CIAE.

References

[1] J. Källne and H. Enge, Magnetic proton recoil spectrometer for fusion plasma neutrons, Nucl. Instr. and Meth. **A 311**(1992)595.

[2] Göran Ericsson, L. Ballabio, S. Conroy et al., Neutron emission spectroscopy at JET—Results from the magnetic proton recoil spectrometer, Rev. of Sci. Instrum., **72**(2001)759.

[3] J.A. Frenje, K.M. Green, D.G. Hicks et al., A neutron spectrometer for precise measurements of DT neutrons from 10 to 18 MeV at OMEGA and the National Ignition Facility, Rev. of Sci. Instrum, **72**(2001)854.

[4] J.A. Frenje, D.T. Casey, C.K. Li et al., First measurements of the absolute neutron spectrum using the magnetic recoil spectrometer at OMEGA, Rev. of Sci. Instrum., **79**, (2008)10E502.

[5] QI Jian-Min, ZHOU Lin and JIANG Shi-Lun, Design and performance analysis of a compact magnetic proton recoil spectrometer for DT neutrons, Chinese Physics C, 2011, 35(4): 374–380.

[6] D. T. Casey J. A. Frenje, M. Gatu Johnson et al., The magnetic recoil spectrometer for measurements of the absolute neutron spectrum at OMEGA and the NIF, Review of Scientific Instruments, **84**(2013)043506.

[7] M. Gatu Johnson, J.A. Frenje, C.K. Li et al., Measurements of fuel and ablator ρR in Symmetry-Capsule implosions with the Magnetic Recoil neutron Spectrometer (MRS) on the National Ignition Facility, Rev. of Sci. Instrum., **85**(2014)11E104.

[8] E.A. Sundén, H. Sjöstranda, S. Conroy et al., The thin-foil magnetic proton recoil neutron spectrometer MPRu at JET, Nucl. Instr. and Meth. **A 610**(2009)682.

[9] M. Tardocchi, S. Conroy, G. Ericsson et al., The monitoring system of a high performance fusion neutron spectrometer, Nucl. Instr. and Meth. **A 485**(2002)624.
[10] H. Sjöstrand, E. A. Sundén, S. Conroy et al., Gain stabilization control system of the upgraded magnetic proton recoil neutron spectrometer at JET, Rev. of Sci. Instrum., **80**, (2009)063505.
[11] Shao-hua Yang, Bin-kang Li, Ming-an Guo et al., Design of 1000 Frame Per-Second High Sensitivity EMCCD Video Processing, International Conference of China Communication and Technology, 2010: 214–217 (in Chinese).
[12] F.J. Beekman and G.A. de Vree, Photon-counting versus an integrating CCD-based gamma camera: important consequences for spatial resolution, Phys. Med. Biol. **50**(2005) N109–N119.